Compressive Sensing Based Direction-of-Arrival Estimation Using Reweighted Greedy Block Coordinate Descent Algorithm for ESPAR Antennas

Hassan Yazdani, Azadeh Vosoughi and Nazanin Rahnavard
University of Central Florida
E-mail: h.yazdani@knights.ucf.edu, azadeh@ucf.edu, nazanin@eecs.ucf.edu

***Abstract*—In this paper, we consider the problem of direction-of-arrival (DoA) estimation using electronically steerable parasitic array radiator (ESPAR) antenna based on compressive sensing. For an ESPAR antenna, the beampatterns and sparse model of DoA estimation problem in terms of overcomplete dictionary and sampling grid is presented. The DoA estimation problem is formulated as a mixed-norm $\ell_{2,1}$ minimization problem and the reactance domain multiple signal classification (RD-MUSIC) spatial spectrum for ESPAR antenna is introduced. Then, we propose reweighted greedy block coordinate descent (RW-GBCD) and reweighted $\ell_{2,1}$-SVD (RW-$\ell_{2,1}$-SVD) algorithms for DOA estimation using ESPAR. The performance of RW-GBCD for DoA estimation is compared to that of GBCD, $\ell_{2,1}$-SVD and RD-MUSIC algorithms. RW-GBCD benefits from less computational complexity compared to RW-$\ell_{2,1}$-SVD. Simulation results demonstrate that the performance of RW-GBCD is better than that of GBCD and $\ell_{2,1}$-SVD. When angle separation is less than 10°, RW-$\ell_{2,1}$-SVD outperforms RW-GBCD. However, when angle separation is more than 10°, the performance of RW-GBCD in terms of root mean square error (RMSE) is approximately the same as that of RW-$\ell_{2,1}$-SVD.**

***Index Terms*—Compressive sensing, direction-of-arrival (DoA), electronically steerable parasitic array radiator (ESPAR), reweighted greedy block coordinate descent (RW-GBCD)**

I. Introduction

Direction-of-arrival (DoA) estimation has been an active research in many fields such as array signal processing, radar, sonar, acoustic and mobile communications. The most popular DoA estimation methods include Beamforming, MUSIC, Capon and ESPRIT [1]. However, the performance of these methods are limited in low SNR or when the sources are placed close to each other.

Since the signal impinging on an antenna array is sparse in the spatial domain, it is possible to employ compressive sensing (CS) for DoA estimation [2]. [3] exploits the sparsity of spatial spectrum of source signals and addresses the problem of source localization for a uniform linear array based on sparse signal recovery. Exploiting ℓ_0 minimization for sparse signal recovery is a complicated combinatorial search problem [4]. The ℓ_1 approximation is a practical alternative for ℓ_0 minimization. The DoA estimation problem is cast to a multiple measurement vector (MMV) problem and ℓ_1-SVD is utilized to recover signal. This MMV problem is solved in [5] using joint ℓ_0 approximation algorithm which essentially is a mixed $\ell_{2,0}$ approximation approach. Authors in [6] and [7] used MUSIC and Capon spectrum, respectively, to design a weighted $\ell_{2,1}$ norm penalty to enhance the recovery performance.

We consider the problem of DoA estimation using electronically steerable parasitic array radiator (ESPAR) antenna which is a reconfigurable antenna utilized for communication purposes [8]. The ESPAR is a circular array comprised of one active element and M parasitic elements. The parasitic elements are short-circuited and loaded by M variable reactors. The ESPAR has gained great attention since it has a single-port output and as a result, the number of phase shifters is reduced significantly. Hence, ESPAR has a simple hardware, is low cost and power efficient. In ESPAR, the parasitic elements are highly coupled to the active element, which requires the element spacing to be small [9]. Therefore, ESPAR has a compact form and it is suitable for mobile user terminals. Signal processing for ESPAR is generally performed in reactance domain instead of element domain [10]. In [10] and [11], authors introduced reactance-domain (RD) MUSIC algorithm for ESPAR antenna and in [12] ℓ_1-SVD is used for CS recovery and DoA estimation.

In this paper, we propose two new algorithms, namely iterative reweighted greedy block coordinate descent (RW-GBCD) and reweighted $\ell_{2,1}$-SVD (RW-$\ell_{2,1}$-SVD) for DoA estimation using ESPAR and compare their performance to that of GBCD and $\ell_{2,1}$-SVD algorithms. The weighted GBCD algorithm with MUSIC prior was originally introduced in [13]. This algorithm provides faster convergence rate compared to $\ell_{2,1}$ norm minimization [13]. We solve GBCD iteratively using the reweighted algorithm to estimate the DoA. Simulation results show that this new method enhances the performance of GBCD and $\ell_{2,1}$-SVD algorithms.

Notation: $vec(\cdot)$ represents the vectorization operator, $\boldsymbol{I}_M$ is an $M \times M$ identity matrix, $(\cdot)^T$ and $(\cdot)^H$ are transpose and conjugate transpose operators, respectively. $diag\{x_1, ..., x_M\}$ is a matrix whose diagonal elements are $x_1, ..., x_M$ and off-diagonal elements are zero and $\|\cdot\|_p$ denotes ℓ_p norm.

II. System Model

We consider an $(M+1)$-element ESPAR as receiver antenna for DoA estimation. The ESPAR is a circular array comprised of one active element (central element) and M parasitic elements symmetrically surrounding the active element and the radius of array is $r < \lambda/2$, where λ is the carrier wavelength.

978-1-5386-0595-0/17/$31.00 ©2017 IEEE

The active element is connected to the single RF chain, while M parasitic elements (which are mutually coupled to the active element) are short-circuited and loaded by M variable reactors (varactors). The reactive loads of parasitic elements are denoted by vector $\boldsymbol{x} = [x_1, ..., x_M]$. Using ESPAR, we can consider a transformation from element-space to beam-space, i.e., we can design the ESPAR beampatterns to divide angular space into M sectors by adjusting reactive loads. For designing the beampatterns, we optimize the reactive loads to maximize the beam gain in a *look direction* (for example 0°) to obtain the 1st beam [14] and we denote it by vector $\boldsymbol{x}_1$. Then, as a result of symmetrical antenna structure, circularly shifting the elements of $\boldsymbol{x}_1$ yields rotated beam to another look direction. With this method, we can obtain a total of M beampatterns. The m-th beampattern for the m-th sector in azimuth plane is expressed as [9]:

$$B_m(\theta) = \boldsymbol{\omega}_m^T \boldsymbol{a}(\theta) \tag{1}$$

where $\boldsymbol{a}(\theta) = [1, e^{-j2\pi \frac{r}{\lambda} cos(\theta - \phi_1)}, ..., e^{-j2\pi \frac{r}{\lambda} cos(\theta - \phi_M)}]^T$ is $(M+1)$-dimensional steering vector of ESPAR antenna, $\phi_m = 2\pi(m-1)/M$ is the angular position of the m-th parasitic elements and $\boldsymbol{\omega}_m = (\boldsymbol{Z} + \boldsymbol{X}_m)^{-1}\boldsymbol{u}$ is the equivalent weight vector for the m-th beampattern [9]. $\boldsymbol{Z}$ is the mutual impedance matrix between elements of ESPAR, $\boldsymbol{u} = [1, 0, ..., 0]^T$ is the $(M+1)$-dimensional selection vector and $\boldsymbol{X}_m$ is a diagonal matrix to form the m-th beam, given by

$$\boldsymbol{X}_m = diag[Z_s \quad j\boldsymbol{x}_m] \tag{2}$$

where Z_s is the impedance of the active element and vector $\boldsymbol{x}_m \in \mathbb{R}^M$ contains reactive loads for m-th beampattern. We note that $\|\boldsymbol{\omega}_m\|_2, \forall m$ are equal. Fig. 1 depicts the beampatterns for a 7-element ESPAR antenna when $r = \lambda/4$.

Assume $K (K \leq M)$ narrowband signals $s_k(t)$ for $k \in \{1, ..., K\}$ from the DoAs θ_k in farfield are impinging on ESPAR. By transforming signals from element-space to beam-space, we can sample signals via different directional beampaterns rather than different elements. We assume that the directions of the K source signals are unchanged during sampling. Applying a set of reactance loads $\boldsymbol{x}_1$, the corresponding measurement $y_1(t)$ will be obtained. Then, by circularly shifting elements of $\boldsymbol{x}_1$, we get $\boldsymbol{x}_2$ and obtain the measurement $y_2(t)$. By repeating this process M times, we can have M measurements. Then, the measurements at time t are written in a vector $\boldsymbol{y}(t) = [y_1(t), y_2(t), ..., y_M(t)]^T$, where the m-th measurement is obtained by using the m-th beampattern and can be written as

$$y_m(t) = \sum_{k=1}^{K} \boldsymbol{\omega}_m^T \boldsymbol{a}(\theta_k) s_k(t) + n_m(t) = \boldsymbol{\omega}_m^T \boldsymbol{A}\boldsymbol{s}(t) + n_m(t) \tag{3}$$

where $\boldsymbol{A} = [\boldsymbol{a}(\theta_1), \boldsymbol{a}(\theta_2), ..., \boldsymbol{a}(\theta_K)]$ is the array manifold matrix, $\boldsymbol{s}(t) = [s_1(t), s_2(t), ..., s_K(t)]^T$ and $n_m(t) \sim CN(0, \sigma_n^2)$ is the additive noise with zero mean and variance σ_n^2. We assume that noises received at different beampatterns are uncorrelated to each other and uncorrelated to the signals. Assuming we have N_s samples of received signal, the observation vector can be written as

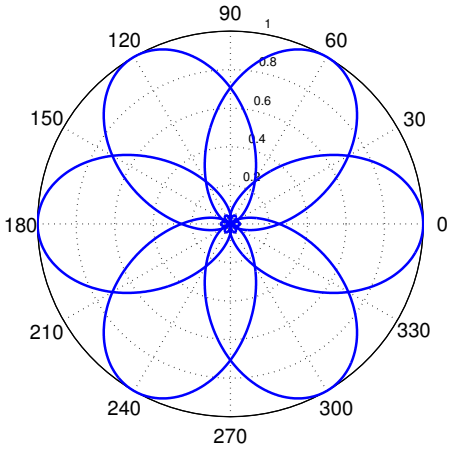

Fig. 1: Beampatterns of a 7-element ESPAR

$$\boldsymbol{y}(t) = \boldsymbol{W}\boldsymbol{A}\boldsymbol{s}(t) + \boldsymbol{n}(t), \qquad \text{for } t = t_1, ..., t_{N_s} \tag{4}$$

where $\boldsymbol{n}(t)$ is the additive noise vector and $\boldsymbol{W} = [\boldsymbol{\omega}_1, \boldsymbol{\omega}_2, ..., \boldsymbol{\omega}_M]^T$ is the projection matrix from element-space to beam-space. Also, $\boldsymbol{W}$ can be considered as mutual coupling matrix (MCM) introduced in [15]. Each row of $\boldsymbol{W}$ is the equivalent weight vector defining one directional beampattern. Then, the covariance matrix of the received signal is given by

$$\boldsymbol{R}_y = \mathbb{E}\left\{\boldsymbol{y}(t)\boldsymbol{y}^H(t)\right\} = \boldsymbol{B}\boldsymbol{R}_s\boldsymbol{B}^H + \sigma_n^2\boldsymbol{I}_M \tag{5}$$

where $\boldsymbol{B} = \boldsymbol{W}\boldsymbol{A}$ and $\boldsymbol{R}_s$ is the diagonal matrix with signals' powers. We stack the N_s measurement vectors and form an $(M \times N_s)$-dimensional received signal as

$$\boldsymbol{Y} = \boldsymbol{B}\boldsymbol{S} + \boldsymbol{N} \tag{6}$$

where $\boldsymbol{Y} = [\boldsymbol{y}(t_1), ..., \boldsymbol{y}(t_{N_s})]$ and $\boldsymbol{S}$ and $\boldsymbol{N}$ can be defined similarly.

III. DoA Estimation

A. Sparse Signal Representation and Problem Statement

We partition the whole azimuth plane into N_θ sampling grids denoted as $\tilde{\boldsymbol{\theta}} = \left[\tilde{\theta}_1, \tilde{\theta}_2, ..., \tilde{\theta}_{N_\theta}\right]$ where $N_\theta \gg K$ and $N_\theta \gg M$. $\tilde{\boldsymbol{\theta}}$ is the set of all potential DoAs and the overcomplete dictionary is thus constructed as $\tilde{\boldsymbol{A}} = \left[\boldsymbol{a}(\tilde{\theta}_1), \boldsymbol{a}(\tilde{\theta}_2), ..., \boldsymbol{a}(\tilde{\theta}_{N_\theta})\right]$. The jointly sparse signal is an $N_\theta \times N_s$ matrix $\tilde{\boldsymbol{S}}$, whose i-th row $\tilde{\boldsymbol{s}}^i$ is nonzero and equal to the k-th source signal $\boldsymbol{s}^k$, when $\tilde{\theta}_i = \theta_k$ ($\boldsymbol{s}^k$ is the k-th row of $\boldsymbol{S}$) . The true support of $\tilde{\boldsymbol{S}}$ is $\Omega = \left\{i \mid \|\tilde{\boldsymbol{s}}^i\|_2 \neq 0\right\}$. Then, the jointly sparse model and the MMV problem is given by

$$\boldsymbol{Y} = \boldsymbol{W}\tilde{\boldsymbol{A}}\tilde{\boldsymbol{S}} + \boldsymbol{N}. \tag{7}$$

In order to reduce both the dimension of $\boldsymbol{Y}$ and sensitivity to noise, we use singular value decomposition (SVD) as

$$\boldsymbol{Y} = \boldsymbol{U}\boldsymbol{L}\boldsymbol{V}^H, \tag{8}$$

where matrices $\boldsymbol{U}$ and $\boldsymbol{V}$ contain eigenvectors of $\boldsymbol{Y}^H\boldsymbol{Y}$ and $\boldsymbol{Y}\boldsymbol{Y}^H$, respectively, $\boldsymbol{L}$ is a diagonal matrix containing

singular values of $\boldsymbol{Y}$ and diagonal elements of $\boldsymbol{L}\boldsymbol{L}^H/N_s$ are eigenvalues of sample covariance matrix $\hat{\boldsymbol{R}}_y = \boldsymbol{Y}\boldsymbol{Y}^H/N_s$. Let $\overline{\boldsymbol{Y}} = \boldsymbol{Y}\boldsymbol{V}\boldsymbol{D}_K$, $\overline{\boldsymbol{S}} = \tilde{\boldsymbol{S}}\boldsymbol{V}\boldsymbol{D}_K$ and $\overline{\boldsymbol{N}} = \boldsymbol{N}\boldsymbol{V}\boldsymbol{D}_K$ where $\boldsymbol{D}_K = [\boldsymbol{I}_K \ \boldsymbol{0}^H]$ and $\boldsymbol{0}$ is a $K \times (Ns - K)$ matrix of zeros. Thus, we have

$$\overline{\boldsymbol{Y}} = \tilde{\boldsymbol{B}}\overline{\boldsymbol{S}} + \overline{\boldsymbol{N}} \tag{9}$$

where $\tilde{\boldsymbol{B}} = \boldsymbol{W}\tilde{\boldsymbol{A}}$. Applying SVD does not change the row support of $\boldsymbol{S}$ and $\overline{\boldsymbol{S}}$ is jointly sparse too. For single measurement vector (SMV) problems, ℓ_0 norm minimization gives the best solution [2]. However, due to its complexity, ℓ_1 relaxation can be used. In the MMV case, the ℓ_1 norm minimization is replaced by mixed-norm $\ell_{2,1}$ norm minimization defined as

$$\min \|\overline{\boldsymbol{S}}\|_{2,1} \qquad \text{s.t. } \|\overline{\boldsymbol{Y}} - \tilde{\boldsymbol{B}}\overline{\boldsymbol{S}}\|_F^2 \leq \epsilon^2 \tag{10}$$

where $\|\overline{\boldsymbol{S}}\|_{2,1} = \sum_{i=1}^{N_\theta} \|\overline{\boldsymbol{s}}^i\|_2$ and $\overline{\boldsymbol{s}}^i$ denotes i-th row of $\overline{\boldsymbol{S}}$. We choose ϵ high enough so that the probability of $\epsilon^2 \leq \|\overline{\boldsymbol{N}}\|_F^2$ is small. Defining an $N_\theta \times 1$ vector $\overline{\boldsymbol{s}}_{(l_2)}$ as

$$\overline{\boldsymbol{s}}_{(l_2)} = \left[\|\overline{\boldsymbol{s}}^1\|_2, ..., \|\overline{\boldsymbol{s}}^{N_\theta}\|_2\right]^T \tag{11}$$

we can write $\|\overline{\boldsymbol{S}}\|_{2,1} = \|\overline{\boldsymbol{s}}_{(l_2)}\|_1$. Finally, the sparse signal can be obtained by minimizing the objective function

$$F(\overline{\boldsymbol{S}}) = \frac{1}{2}\|\overline{\boldsymbol{Y}} - \tilde{\boldsymbol{B}}\overline{\boldsymbol{S}}\|_F^2 + \zeta\|\overline{\boldsymbol{s}}_{(l_2)}\|_1 \tag{12}$$

where the parameter ζ controls the trade-off between the residual norm and the sparsity of the signal. A theoretical guidance for choosing an appropriate ζ is presented in [7] and [13]. This problem can be solved using second order cone programming (SOCP), instead of nonlinear optimization, since SOCP has efficient numerical solution. Finally, the normalized spatial spectrum is

$$P(\theta_i) = \frac{|\overline{s}^i_{(l_2)}|^2}{\max\left\{|\overline{s}^i_{(l_2)}|^2\right\}}, \qquad \text{for } i = 1, 2, ..., N_\theta \tag{13}$$

where $\overline{s}^i_{(l_2)}$ is the i-th row of vector $\overline{s}_{(l_2)}$ and the K-largest values of $P(\theta_i)$ represent the estimates of DoAs.

The ℓ_0 and ℓ_1 norms of a vector are equal when the absolute value of every element is either 0 or 1. In other words, ℓ_1 norm depends on magnitude of vector's elements which may cause performance degrading. If we can somehow scale the non-zero elements, then ℓ_0 and ℓ_1 can get close and CS recovery performance will be better. Thus, our goal is finding weighting coefficients γ_i so that $\|\Gamma\overline{\boldsymbol{s}}_{(l_2)}\|_1$ get close to $\|\overline{\boldsymbol{s}}_{(l_2)}\|_0$, where $\boldsymbol{\Gamma} = diag\{\gamma_1, ..., \gamma_{N_\theta}\}$.

In [16], an iterative reweighted ℓ_1 algorithm is introduced in which large weights are appointed to those elements of vector $\overline{\boldsymbol{s}}_{(l_2)}$ whose indices are more likely to be outside of the support. We use a modified version of the method introduced in [16] and propose reweighted $\ell_{2,1}$-SVD (RW-$\ell_{2,1}$-SVD) method. In this method, we use reactance-domain MUSIC algorithm to form the first weighting vector $\boldsymbol{\gamma}^{(1)} = [\gamma_1^{(1)}, ..., \gamma_{N_\theta}^{(1)}]$ as follows.

Applying eigenvalue decomposition, the covariance $\boldsymbol{R}_y$ can be written as $\boldsymbol{R}_y = \sum_{i=1}^{M} \eta_i \boldsymbol{e}_i \boldsymbol{e}_i^H$, where $\boldsymbol{e}_i$ is eigenvector corresponding to eigenvalue η_i. Let $\boldsymbol{\Lambda}_s = [\boldsymbol{e}_1, ..., \boldsymbol{e}_K]$ and $\boldsymbol{\Lambda}_n = [\boldsymbol{e}_{K+1}, ..., \boldsymbol{e}_M]$ represent signal and noise subspaces, respectively. Since signal and noise subspaces are orthogonal, we can write $\boldsymbol{\Lambda}_n^H \tilde{\boldsymbol{B}}_\Omega = \boldsymbol{0}$, where $\tilde{\boldsymbol{B}}_\Omega$ is true manifold matrix, i.e., $\tilde{\boldsymbol{B}}_\Omega = \boldsymbol{B}$. Then, the MUSIC spatial spectrum for the ESPAR antenna is given by

$$P_M(\theta_i) = \frac{1}{\|\boldsymbol{\Lambda}_n^H \tilde{\boldsymbol{b}}_i\|_2^2}, \qquad \text{for } i = 1, 2, ..., N_\theta \tag{14}$$

where $\tilde{\boldsymbol{b}}_i$ is the i-th column of $\tilde{\boldsymbol{B}}$. The K-largest values of MUSIC spectrum are estimates of DoAs $\theta_k, k \in \{1, ..., K\}$ using MUSIC algorithm. Since $P_M(\theta_i) \gg P_M(\theta_j), \ \forall i \in \Omega$ and $\forall j \in \Omega^c$, by choosing the elements of weighing vector for first iteration as $\gamma_i^{(1)} = \|\boldsymbol{\Lambda}_n^H \tilde{\boldsymbol{b}}_i\|_2$, the elements of signal vector whose index are outside of true support Ω are penalized by a larger weight. Next, for τ-th $(2 \leq \tau \leq \tau_{max})$ iteration of RW-$\ell_{2,1}$-SVD algorithm, we set

$$\gamma_i^{(\tau)} = \frac{1}{\overline{s}^{(\tau-1),i}_{(l_2)} + \delta}, \quad \text{for } \tau = 2, ..., \tau_{max} \text{ and } i = 1, ..., N_\theta \tag{15}$$

where $\overline{s}^{(\tau)}_{(l_2)}$ is the solution of optimization problem $\frac{1}{2}\|\overline{\boldsymbol{Y}} - \tilde{\boldsymbol{B}}\overline{\boldsymbol{S}}\|_F^2 + \zeta\|\boldsymbol{\Gamma}^{(\tau)}\overline{\boldsymbol{s}}^{(\tau)}_{(l_2)}\|_1$ for iteration τ, $\overline{s}^{(\tau),i}_{(l_2)}$ is then i-th element of vector $\overline{\boldsymbol{s}}^{(\tau)}_{(l_2)}$, $\boldsymbol{\Gamma}^{(\tau)} = diag\{\gamma_1^{(\tau)}, ..., \gamma_{N_\theta}^{(\tau)}\}$ and $\delta > 0$ is a small number.

B. Reweighted Greedy Block Coordinate Descent Algorithm

In this section we propose the reweighted greedy block coordinate descent (RW-GBCD) algorithm for DoA estimation using ESPAR antenna. The standard block coordinate descent (BCD) algorithm is an iterative algorithm which builds a quadratic approximation for $G(\overline{\boldsymbol{S}}) = \frac{1}{2}\|\overline{\boldsymbol{Y}} - \tilde{\boldsymbol{B}}\overline{\boldsymbol{S}}\|_F^2$. Then, the approximation of objective function $F(\overline{\boldsymbol{S}})$ for iteration $j \in \{1, ..., j_{max}\}$ is written as [13]

$$\begin{aligned} F_a(\overline{\boldsymbol{S}}) &= G\left(\overline{\boldsymbol{S}}(j)\right) + vec\left(\nabla G\left(\overline{\boldsymbol{S}}(j)\right)\right)^H vec\left(\overline{\boldsymbol{S}} - \overline{\boldsymbol{S}}(j)\right) \\ &\quad + \frac{1}{2\beta}\|\overline{\boldsymbol{S}} - \overline{\boldsymbol{S}}(j))\|_F^2 + \zeta\|\overline{\boldsymbol{S}}\|_{2,1} \\ &= \sum_{i=1}^{M}\left\{\frac{1}{2\beta}\|\overline{\boldsymbol{s}}^i - \boldsymbol{p}^i\|_2^2 + \zeta\|\overline{\boldsymbol{s}}^i\|_2\right\} + c(j) \end{aligned} \tag{16}$$

where $\nabla G\left(\overline{\boldsymbol{S}}(j)\right) = \tilde{\boldsymbol{B}}^H\left(\tilde{\boldsymbol{B}}\overline{\boldsymbol{S}}(j) - \overline{\boldsymbol{Y}}\right)$ and $c(j) = G\left(\overline{\boldsymbol{S}}(j)\right) - \frac{\beta}{2}\|\nabla G\left(\overline{\boldsymbol{S}}(j)\right)\|_F^2$. Vectors $\overline{\boldsymbol{s}}^i$ and $\boldsymbol{p}^i$ are the i-th row of $\overline{\boldsymbol{S}}$ and $\boldsymbol{P}(j)$, respectively, where $\boldsymbol{P}(j) = \overline{\boldsymbol{S}}(j) - \beta\nabla G\left(\overline{\boldsymbol{S}}(j)\right)$ and $\beta = 1/\|\tilde{\boldsymbol{b}}_i\|_2^2$. The BCD algorithm minimizes (16) to update $\overline{\boldsymbol{S}}(j+1)$. Optimization problem (16) is separable and the solution to the i-th sub-problem, $i = 1, ..., N_\theta$, is

$$\overline{\boldsymbol{s}}^i(j+1) = \frac{\boldsymbol{p}^i(j)}{\|\boldsymbol{p}^i(j)\|_2}\max\left(0, \|\boldsymbol{p}^i(j)\|_2 - \zeta\beta\right). \tag{17}$$

In contrast to the BCD, in the τ-th iteration of RW-GBCD algorithm *only* the block that yields the greatest descent distance $\Delta d_i = \|\overline{\boldsymbol{s}}^i(j+1) - \overline{\boldsymbol{s}}^i(j)\|_2/\gamma_i^{(\tau)}$ will be updated. Suppose i_0-th block yields the greatest Δd_i, i.e.,

$$i_0 = \arg\max_i \{\Delta d_i\} \tag{18}$$

Then, we only update $\overline{\boldsymbol{s}}^{i_0}(j+1)$ using (17), while $\overline{\boldsymbol{s}}^i(j+1) = \overline{\boldsymbol{s}}^i(j), i \neq i_0$. The RW-GBCD algorithm is summarized in Algorithm 1.

Algorithm 1: Proposed RW-GBCD algorithm

for $\tau = 1, ..., \tau_{max}$ **do**

1: **if** $\tau = 1$ **then**

$\gamma_i^{(1)} = \|\boldsymbol{\Lambda}_n^H \tilde{\boldsymbol{b}}_i\|_2$

else

$\gamma_i^{(\tau)} = 1/\left(\overline{s}_{(l_2)}^{(\tau-1),i} + \delta\right)$

end

2: set $\overline{\boldsymbol{S}}(0) = \boldsymbol{0}$

3: **for** $j = 1, ..., j_{max}$ **do**

3-1: $\boldsymbol{Q} \leftarrow \overline{\boldsymbol{S}}(k-1)$

3-2: $\boldsymbol{P} = \boldsymbol{Q} - \beta \tilde{\boldsymbol{B}}^H \left(\tilde{\boldsymbol{B}}\boldsymbol{Z} - \overline{\boldsymbol{Y}}\right)$

3-3: **for** $i = 1 : N_\theta$ **do**

$\overline{\boldsymbol{s}}^i(j) = \frac{\boldsymbol{p}^i}{\|\boldsymbol{p}^i\|_2} \max\left(0, \|\boldsymbol{p}^i\|_2 - \zeta\beta\right)$

$\Delta d_i = \frac{1}{\gamma_i^{(\tau)}} \|\overline{\boldsymbol{s}}^i(j) - \boldsymbol{q}^i\|_2$

end

3-4: $i_0 =$ arg max $\{\Delta d_i\}$

3-5: $\overline{\boldsymbol{S}}(j) \leftarrow [\boldsymbol{q}^1; ...; \boldsymbol{q}^{i_0-1}; \overline{\boldsymbol{s}}^{i_0}(j); \boldsymbol{q}^{i_0+1}; ...; \boldsymbol{q}^{N_\theta}]$

end

4: $\overline{s}_{(l_2)}^{(\tau)} \leftarrow \ell_2$ norm of rows of $\overline{\boldsymbol{S}}(j_{max})$

end

IV. Numerical Results

In this section, we numerically evaluate the performance of RW-GBCD and RW-$\ell_{2,1}$-SVD algorithms. The ESPAR antenna has 7 elements, the radius is $r = \lambda/4$ and the reactance load for first beampattern is $\boldsymbol{x}_1 = [31.2, 57.03, -67.55, -67.55, 57.03, 31.2]$. Suppose two narrowband uncorrelated sources located at DoAs $\boldsymbol{\theta} = [-10°, 5°]$ in farfield, the sources transmit signal with unit power and noise variance is $\sigma_n^2 = 0.01$. We divide azimuth plane into $N_\theta = 1800$ grids with $0.1°$ resolution and the ESPAR gathers $N_s = 400$ samples. The RW-$\ell_{2,1}$-SVD is solved by CVX toolbox [17]. In our simulations, $\delta = 0.1$, $\zeta = 3$ and $\tau_{max} = 3$.

In Fig. 2 the normalized spatial spectrum of RD-MUSIC, GBCD and $\ell_{2,1}$-SVD are shown. The recovered signal by GBCD algorithm has only few nonzero rows (support) and its spatial spectrum is not continuous. The 2-largest values of spatial spectrum for RD-MUSIC, GBCD and $\ell_{2,1}$-SVD are located at directions $[4.9°, 5°]$, $[-1.2°, -1.1°]$ and $[-27°, 1.9°]$, respectively. Also, there is a large peak (spike) at direction $90°$ for GBCD and $\ell_{2,1}$-SVD. It can be seen that RD-MUSIC, GBCD and $\ell_{2,1}$-SVD cannot estimate the DoAs exactly.

The spatial spectrum for first iteration of proposed reweighted algorithms is shown in Fig. 3. The 2-largest values of spatial spectrum for first iteration of RW-GBCD and RW-$\ell_{2,1}$-SVD are located at directions $[4.8°, 4.9°]$ and $[-10.5°, 4.8°]$, respectively. These curves are zoomed in Fig. 4. It can be seen from Fig. 4 that nonzero elements of recovered signal by RW-GBCD are gathered around the true DoAs. Moreover, the large spike in $90°$ has been removed. In Fig. 5, the spatial spectrum for last (third) iteration is shown. The DoA estimate using RW-GBCD and RW-$\ell_{2,1}$-SVD are $[-10.9°, 4.9°]$ and $[-10.5°, 4.8°]$, respectively. We can see that in the third iteration, only two nonzero row (support) of

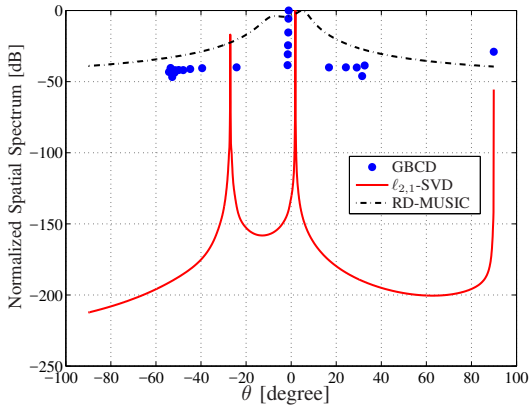

Fig. 2: Normalized spatial spectrum of RD-MUSIC, GBCD and $\ell_{2,1}$-SVD.

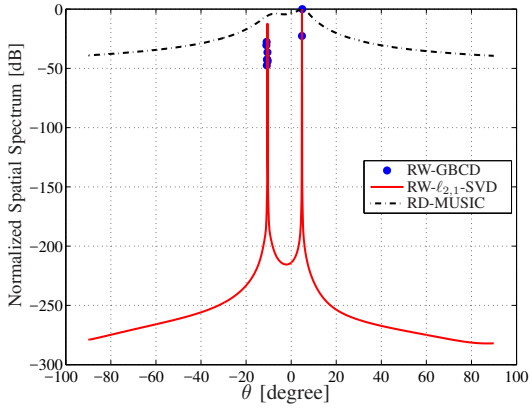

Fig. 3: Normalized spatial spectrum of RD-MUSIC, RW-GBCD and RW-$\ell_{2,1}$-SVD for first iteration.

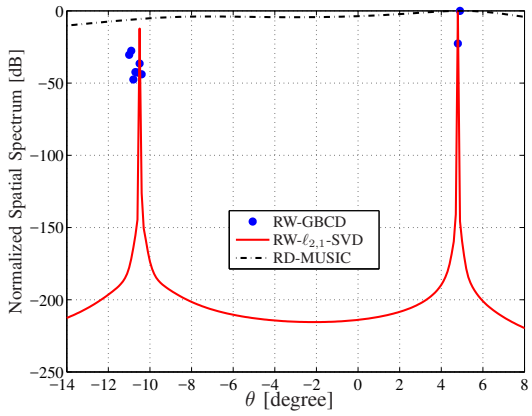

Fig. 4: Normalized spatial spectrum of RD-MUSIC, RW-GBCD and RW-$\ell_{2,1}$-SVD for first iteration.

recovered signal using RW-GBCD is maintained. To compare the accuracy of RW-GBCD and RW-$\ell_{2,1}$-SVD, the root mean square error (RMSE) defined as

$$RMSE = \sqrt{\sum_{n=1}^{N_{mont}} \sum_{k=1}^{K} \frac{\left(\tilde{\theta}_k(n) - \theta_k\right)^2}{K N_{mont}}} \qquad (19)$$

versus angle separation $\Delta\theta$ for $N_{mont} = 500$, when sources are located at DoAs $[-10, 5 + \Delta\theta]$ is shown in Fig. 6. It

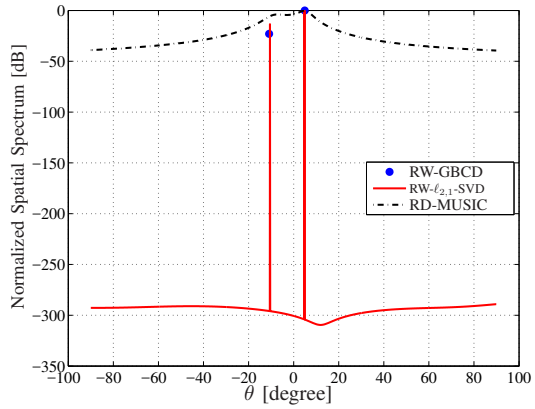

Fig. 5: Normalized spatial spectrum of RD-MUSIC, RW-GBCD and RW-$\ell_{2,1}$-SVD for last iteration.

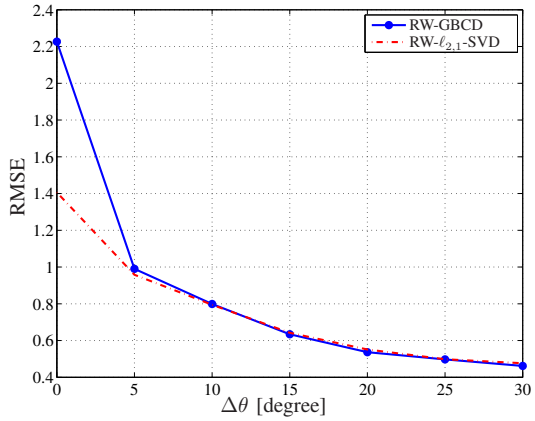

Fig. 6: RMSE of RW-GBCD and RW-$\ell_{2,1}$-SVD versus $\Delta\theta$.

can be seen that for $\Delta\theta < 10°$, RW-$\ell_{2,1}$-SVD outperforms RW-GBCD. However, for $\Delta\theta > 10°$, two methods have approximately the same value of RMSE.

V. Conclusion

In this paper, we proposed the RW-GBCD and RW-$\ell_{2,1}$-SVD algorithms for DOA estimation using ESPAR antennas. We presented the beampatterns and sparse model of DoA estimation problem in terms of overcomplete dictionary and sampling grid. We formulated the DoA estimation problem as a mixed-norm $\ell_{2,1}$ minimization problem and introduced the RD-MUSIC algorithm. RW-GBCD benefits from less computational complexity compared to RW-$\ell_{2,1}$-SVD. Our simulation results showed that the performance of RW-GBCD is better than that of GBCD and $\ell_{2,1}$-SVD. When $\Delta\theta$ is less than 10°, RW-$\ell_{2,1}$-SVD outperforms RW-GBCD. However, for $\Delta\theta \geq 10°$, the performance of RW-GBCD in terms of RMSE is approximately the same as that of RW-$\ell_{2,1}$-SVD.

Acknowledgment

This research is supported by NSF under grants ECCS-1443942 and ECCS-1418710.

References

[1] H. Krim and M. Viberg, "Two decades of array signal processing research: the parametric approach," *IEEE Signal Processing Magazine*, vol. 13, no. 4, pp. 67–94, Jul 1996.

[2] E. J. Candes and M. B. Wakin, "An introduction to compressive sampling," *IEEE Signal Processing Magazine*, vol. 25, no. 2, pp. 21–30, March 2008.

[3] D. Malioutov, M. Cetin, and A. S. Willsky, "A sparse signal reconstruction perspective for source localization with sensor arrays," *IEEE Transactions on Signal Processing*, vol. 53, no. 8, pp. 3010–3022, Aug 2005.

[4] M. Joneidi, A. Zaeemzadeh, N. Rahnavard, and M. B. Khalilsarai, "Matrix coherency graph: A tool for improving sparse coding performance," in *2015 International Conference on Sampling Theory and Applications (SampTA)*, May 2015, pp. 168–172.

[5] M. M. Hyder and K. Mahata, "Direction-of-arrival estimation using a mixed $\ell_{2,0}$ norm approximation," *IEEE Transactions on Signal Processing*, vol. 58, no. 9, pp. 4646–4655, Sept 2010.

[6] C. Zheng, G. Li, Y. Liu, and X. Wang, "Subspace weighted $\ell_{2,1}$ minimization for sparse signal recovery," *EURASIP Journal on Advances in Signal Processing*, vol. 2012, no. 1, p. 98, 2012. [Online]. Available: http://dx.doi.org/10.1186/1687-6180-2012-98

[7] X. Xu, X. Wei, and Z. Ye, "DoA estimation based on sparse signal recovery utilizing weighted ℓ_1-norm penalty," *IEEE Signal Processing Letters*, vol. 19, no. 3, pp. 155–158, March 2012.

[8] M. Shirazi and X. Gong, "Singly-polarized reconfigurable slot-ring antenna/array with fractal shapes," in *2016 IEEE International Symposium on Antennas and Propagation (APSURSI)*, June 2016, pp. 843–844.

[9] C. Sun, A. Hirata, T. Ohira, and N. C. Karmakar, "Fast beamforming of electronically steerable parasitic array radiator antennas: theory and experiment," *IEEE Transactions on Antennas and Propagation*, vol. 52, no. 7, pp. 1819–1832, July 2004.

[10] C. Plapous, J. Cheng, E. Taillefer, A. Hirata, and T. Ohira, "Reactance domain music algorithm for ESPAR antennas," in *2003 33rd European Microwave Conference*, Oct 2003, pp. 793–796.

[11] R. Qian, M. Sellathurai, and T. Ratnarajah, "Directional spectrum sensing for cognitive radio using ESPAR arrays with a single RF chain," in *2014 European Conference on Networks and Communications (EuCNC)*, June 2014, pp. 1–5.

[12] R. Qian, M. Sellathurai, and J. Chambers, "Direction-of-arrival estimation with single-RF ESPAR antennas via sparse signal reconstruction," in *2015 IEEE 16th International Workshop on Signal Processing Advances in Wireless Communications (SPAWC)*, June 2015, pp. 485–489.

[13] X. Wei, Y. Yuan, and Q. Ling, "DoA estimation using a greedy block coordinate descent algorithm," *IEEE Transactions on Signal Processing*, vol. 60, no. 12, pp. 6382–6394, Dec 2012.

[14] D. Wilcox, E. Tsakalaki, A. Kortun, T. Ratnarajah, C. B. Papadias, and M. Sellathurai, "On spatial domain cognitive radio using single-radio parasitic antenna arrays," *IEEE Journal on Selected Areas in Communications*, vol. 31, no. 3, pp. 571–580, March 2013.

[15] R. Goossens and H. Rogier, "A hybrid UCA-RARE/Root-MUSIC approach for 2-D direction of arrival estimation in uniform circular arrays in the presence of mutual coupling," *IEEE Transactions on Antennas and Propagation*, vol. 55, no. 3, pp. 841–849, March 2007.

[16] E. J. Candès, M. B. Wakin, and S. P. Boyd, "Enhancing sparsity by reweighted ℓ_1 minimization," *Journal of Fourier Analysis and Applications*, vol. 14, no. 5, pp. 877–905, 2008. [Online]. Available: http://dx.doi.org/10.1007/s00041-008-9045-x

[17] M. Grant and S. Boyd, "CVX: Matlab software for disciplined convex programming, version 2.1," http://cvxr.com/cvx, Mar. 2014.